STEM CELLS TRANSLATIONAL MEDICINE®

TISSUE ENGINEERING AND REGENERATIVE MEDICINE

An Abundant Perivascular Source of Stem Cells for Bone Tissue Engineering

AARON W. JAMES,[a,b,c*] JANETTE N. ZARA,[b*] MIRKO CORSELLI,[b] ASAL ASKARINAM,[a] ANN M. ZHOU,[a] ALIREZA HOURFAR,[a] ALAN NGUYEN,[a] SILVA MEGERDICHIAN,[a] GREG ASATRIAN,[a] SHEN PANG,[a] DAVID STOKER,[d,e] XINLI ZHANG,[a] BENJAMIN WU,[f] KANG TING,[a,b] BRUNO PÉAULT,[b,g] CHIA SOO[b]

Key Words. Adult stem cells • CD34+ • Cell biology • Cell surface markers • Cell transplantation • Cellular therapy • Mesenchymal stem cells • Osteoblast

ABSTRACT

Adipose tissue is an ideal mesenchymal stem cell (MSC) source, as it is dispensable and accessible with minimal morbidity. However, the stromal vascular fraction (SVF) of adipose tissue is a heterogeneous cell population, which has disadvantages for tissue regeneration. In the present study, we prospectively purified human perivascular stem cells (PSCs) from $n = 60$ samples of human lipoaspirate and documented their frequency, viability, and variation with patient demographics. PSCs are a fluorescence-activated cell sorting-sorted population composed of pericytes (CD45−, CD146+, CD34−) and adventitial cells (CD45−, CD146−, CD34+), each of which we have previously reported to have properties of MSCs. Here, we found that PSCs make up, on average, 43.2% of SVF from human lipoaspirate (19.5% pericytes and 23.8% adventitial cells). These numbers were minimally changed by age, gender, or body mass index of the patient or by length of refrigerated storage time between liposuction and processing. In a previous publication, we observed that human PSCs (hPSCs) formed significantly more bone in vivo in comparison with unsorted human SVF (hSVF) in an intramuscular implantation model. We now extend this finding to a bone injury model, observing that purified hPSCs led to significantly greater healing of mouse critical-size calvarial defects than hSVF (60.9% healing as opposed to 15.4% healing at 2 weeks postoperative by microcomputed tomography analysis). These studies suggest that adipose-derived hPSCs are a new cell source for future efforts in skeletal regenerative medicine. Moreover, hPSCs are a stem cell-based therapeutic that is readily approvable by the U.S. Food and Drug Administration, with potentially increased safety, purity, identity, potency, and efficacy. STEM CELLS TRANSLATIONAL MEDICINE *2012;1:673–684*

INTRODUCTION

Adipose-derived stromal cells (ASCs) have been shown to lead to successful healing of both small animal [1, 2] and large animal [3] skeletal defects; however, ASCs are defined only by adherence to standard culture plates. This in vitro culture and expansion allows for a relative purification (rapid changes in cell surface markers are observed in culture of ASCs) [4, 5] but gives no information on the native identity of ASCs in situ and also introduces the possibility of immunogenicity, infection, and genetic instability [6, 7]. In this regard, the direct isolation and immediate application of stem cells (bypassing any culture period) would be highly advantageous from the standpoints of safety and practicality. A number of investigators have attempted this, using freshly isolated total stromal vascular fraction (SVF) from adipose tissue (SVF is the total cellular yield after collagenase digestion and centrifugation). However, available studies using unpurified SVF show poor and unreliable bone formation [8] or lower bone regeneration efficacy relative to cultured ASCs [9]. This lowered utility for bone regeneration can best be attributed to the highly heterogeneous nature of SVF, which includes non-mesenchymal stem cell (MSC) types, such as inflammatory cells, hematopoietic cells, and endothelial cells, among others [10]. Thus, for efforts in tissue engineering, the need to purify MSCs is readily apparent. The purification of freshly isolated SVF based on cell surface markers would allow for rapid isolation of cells, bypass time-consuming culture expansion, and yield a cell population of high purity that may be safer and more efficacious for bone regeneration.

Our laboratory has previously reported on the MSC characteristics of cells that are intimately associated with the vasculature, termed perivascular stem cells (PSCs). PSCs are found in every vascularized organ and are composed of two known populations associated with blood vessels [11–15]. These distinct perivascular MSC populations are isolatable by multicolor fluorescence-activated cell sorting (FACS). These include CD45−, CD146+, CD34− pericytes surrounding microvessels and capillaries [11, 16]

[a]Dental and Craniofacial Research Institute and Section of Orthodontics, School of Dentistry, [b]UCLA and Orthopaedic Hospital Department of Orthopaedic Surgery and the Orthopaedic Hospital Research Center, [c]Department of Pathology and Laboratory Medicine, David Geffen School of Medicine, and [f]Department of Bioengineering, University of California, Los Angeles, Los Angeles, California, USA; [d]Private practice, Marina del Rey, California, USA; [e]Division of Plastic and Reconstructive Surgery, University of Southern California, Los Angeles, California, USA; [g]Center For Cardiovascular Science and MRC Center for Regenerative Medicine, University of Edinburgh, Edinburgh, United Kingdom

*Contributed equally as first authors.

Correspondence: Kang Ting, D.M.D., D.Med.Sci., Box 951668, 30-113 CHS, 10833 Le Conte Avenue, Los Angeles, California 90095, USA. Telephone: 310-206-6305; Fax: 310-206-5349; e-mail: kting@dentistry.ucla.edu; or Bruno Péault, Ph.D., 615 Charles E. Young Drive South, Room 410, Los Angeles, California 90095, USA. Telephone: 310-794-1339; Fax: 310-825-5409; e-mail: bpeault@mednet.ucla.edu; or Chia Soo, M.D., Department of Orthopaedic Surgery, University of California, Los Angeles, 675 Charles E. Young Drive South, MRL 2641A, Los Angeles, California 90095-1579, USA. Telephone: 310-794-5479; Fax: 310-206-7783; e-mail: bsoo@ucla.edu

Received May 9, 2012; accepted for publication July 5, 2012; first published online in SCTM *EXPRESS* September 5, 2012.

1066-5099/2012/$20.00/0

http://dx.doi.org/10.5966/sctm.2012-0053

and a second distinct CD45−, CD146−, CD34+ adventitial cell type, associated with larger blood vessels [17]. Both cell types are obtainable from human adipose tissue and resemble MSCs in morphology, growth, surface markers, and clonal multilineage differentiation potential [11–15]. Other research groups have attempted to purify SVF for tissue regeneration and have successfully enriched for osteoprogenitor [18] and chondroprogenitor [19] cell types—but importantly not for multipotent MSCs. In our most recent report, we compared the bone-forming potential of human SVF (hSVF) with that of human PSCs (hPSCs) purified from identical patient samples [20]. Using an intramuscular implantation model, we found evidence that hPSCs outperform hSVF in osteogenic differentiation and bone formation [20]. This was also accompanied by increased expression of bone morphogenetic protein 2 (BMP2), BMP7, and vascular endothelial growth factor (VEGF) (A. Askarinam, A.W. James, J.N. Zara, manuscript in preparation). These data led us to conclude that hPSCs show a clear regenerative advantage over an unpurified stromal cell population.

In this study, we first prospectively purified hPSCs from $n = 60$ samples of lipoaspirate and documented their frequency, viability, and variation with patient demographics. We observed that the isolation of hPSCs from lipoaspirate is a highly reproducible process, with minimal variation. Next, we used a mouse calvarial defect model to compare the bone healing potential of purified hPSCs with that of unsorted hSVF. In this manner, we documented hPSCs as a highly reproducible and efficacious cell source for bone tissue regeneration.

Materials and Methods

Isolation of Stromal Vascular Fraction from Human Lipoaspirate

Human lipoaspirate ($n = 60$ donors) was obtained from patients undergoing cosmetic liposuction. Age, gender, and body mass index (BMI) of each patient were recorded. No patient identifiers were obtained, and therefore no University of California, Los Angeles, institutional review board approval was required [45 CFR 46.102(f)]. Lipoaspirate was stored at 4°C before processing; length of time in refrigerated storage was recorded for all specimens. The hSVF fraction was obtained by collagenase digestion as per a prior publication [17]. Briefly, lipoaspirate was diluted with an equal volume of phosphate-buffered saline (PBS) before digestion with Dulbecco's modified Eagle's medium (DMEM) containing 3.5% bovine serum albumin (Sigma-Aldrich, St. Louis, MO, http://www.sigmaaldrich.com) and 1 mg/ml collagenase type II for 70 minutes under agitation at 37°C. Adipocytes were separated and removed by centrifugation. The pellet was resuspended in red-cell lysis buffer (155 mM NH_4Cl, 10 mM $KHCO_3$, and 0.1 mM EDTA) and incubated for 10 minutes at room temperature. After centrifugation, pellets were resuspended in PBS and filtered at 70 μm. The resulting hSVF was either further processed for cell sorting (to isolate PSCs) or seeded immediately onto scaffolds for in vivo application. In order to calculate live cell number for implantation, trypan blue staining was performed to assess cell viability. Demographics for those patient samples used for in vivo studies ($n = 4$) are presented in supplemental online Table 1.

Purification of Perivascular Stem Cells from Human SVF

PSCs were purified by FACS from the hSVF as previously described [17]. hSVF was incubated with a mixture of the following directly conjugated antibodies: anti-CD34-APC (1:100; BD Biosciences, San Diego, CA, http://www.bdbiosciences.com), anti-CD45-APC-cy7 (1:100; BD Biosciences), and anti-CD146-FITC (1:100; AbD Serotec, Raleigh, NC, http://www.ab-direct.com). All incubations were performed at 4°C for 15 minutes in the dark. Before sorting, 4′,6-diamidino-2-phenylindole (DAPI) (1:1,000; Invitrogen, Carlsbad, CA, http://www.invitrogen.com) was added for dead cell exclusion. The solution was then passed through a 70-μm cell filter and then run on a FACSAria cell sorter (BD Biosciences). Sorted cells were used for in vivo application immediately or plated for in vitro studies. In this manner, distinct microvessel pericytes (CD45−, CD146+, CD34−) and adventitial cells (CD45−, CD146−, CD34+) were isolated and combined to constitute the PSC population.

Demographic Analysis

Parameters from isolation and purification of PSCs were recorded, including the total cell yield (expressed as total SVF cell number per 100 ml of tissue lipoaspirate), the cell viability (percentage of DAPI− cells), percentage of hematopoietic cells (percentage of CD45+ cells), percentage of pericytes (percentage of CD45−, CD146+, CD34− cells), percentage of adventitial cells (percentage of CD45−, CD146−, CD34+, cells), and percentage of PSCs (percentage of pericytes + adventitial cells). Demographics of each patient were obtained, including age, gender, and BMI. Parameters were stratified by each demographic parameter, as well as by cold-storage time at 4°C between isolation and processing.

Scaffold Fabrication

Apatite-coated poly(lactic-coglycolic acid) (PLGA) scaffolds were fabricated as previously described [1], from 85/15 poly(lactic-coglycolic acid) (inherent viscosity = 0.61 dl/g; Birmingham Polymers, Pelham, AL, http://www.durect.com) by solvent casting and a particulate leaching process. Briefly, PLGA/chloroform solutions were mixed with 200–300-μm-diameter sucrose to obtain 92% porosity (volume fraction) and compressed into thin sheets in a nonstick mold. After freeze-drying overnight, scaffolds were immersed in three changes of double-distilled water (ddH_2O) to dissolve the sucrose and gently removed from the nonstick plate with a fine-tip spatula. After particulate leaching, all scaffolds were disinfected by immersion in 50%, 60%, and 70% ethanol for 30 minutes each, followed by three rinses in ddH_2O. All scaffolds were then dried under a laminar flow hood.

Surgical Procedures

Calvarial defects were performed as previously described with some modification [1]. Nonhealing, critical-sized (3-mm) calvarial defects were created in the right parietal bone of adult SCID mice (Charles River Laboratories, Wilmington, MA, http://www.criver.com) using a high-speed dental drill. Procedures were performed under isoflurane sedation. After cleaning the site with alternating scrubs of Betadine and alcohol, an incision was made just off the sagittal midline to expose the right parietal bone. The pericranium was removed with a sterile cotton swab. Using diamond-coated trephine bits, and under saline irrigation, unilateral full-thickness calvarial defects were created in the non-suture-associated parietal bone. Particular care was made not to

injure the underlying dura mater, as this tissue has been demonstrated to be critical for normal stem cell-mediated calvarial regeneration [21].

In preparation for scaffold implantation, scaffolds were seeded with hSVF or hPSCs. Two hundred fifty thousand cells from each individual patient sample were resuspended in 25 μl of growth medium (DMEM, 10% fetal bovine serum, 1% penicillin/streptomycin) and placed directly onto the scaffold for 30 minutes (25 μl of medium without cells was used for empty scaffold controls). The scaffolds were subsequently submerged in 100 μl of growth medium for 8 hours of incubation. Before implantation, cell-seeded scaffolds were rinsed in sterile PBS to prevent transfer of medium-derived growth factors or immunogens. Animals were split equally into three treatment groups: (a) scaffold only, in which a PLGA scaffold without cells was placed in the defect site ($n = 18$ mice); (b) scaffold + hSVF ($n = 16$ mice split equally from $n = 4$ separate patient samples); and (c) scaffold + hPSCs ($n = 16$ mice split equally from $n = 4$ separate patient samples). Finally, the skin was sutured with 6-0 vicryl, and animals were monitored per established postoperative animal care protocols.

Radiographic Imaging

Calvarial defects were analyzed by live microcomputed tomography (microCT) from 0 to 8 weeks postoperative as previously described, under isoflurane sedation [22]. A non-contrast-enhanced microCT study using a microCAT II (Siemens Preclinical Solutions, Malvern, PA, http://www.medical.siemens.com) imaging system was used to scan animals with a 20-minute acquisition time. MicroCT images were created using Feldkamp reconstruction at a 200-μm resolution. Data were analyzed and quantified by AMIDE (A Medical Image Data Examiner; http://amide.sourceforge.net) software.

High-resolution, post-mortem microCT scanning was performed at 8 weeks postoperative. After formalin fixation, samples were imaged using high-resolution microCT (Skyscan 1172F; Skyscan, Kontich, Belgium, http://www.skyscan.be) at an image resolution of 19.73 μm and analyzed using the DataViewer, Recon, CTAn, and CTVol software provided by the manufacturer. Threshold values for three-dimensional (3D) reconstructions can be found in the figure legends.

Histology and Immunohistochemistry

After radiographic analysis, samples were decalcified in 19% EDTA and embedded in paraffin. Hematoxylin/eosin (H&E) staining and Masson's trichrome staining were performed. Immunohistochemistry was performed with primary antibodies against osteopontin (OPN) (Santa Cruz Biotechnology Inc., Santa Cruz, CA, http://www.scbt.com), osteocalcin (OCN) (Santa Cruz Biotechnology), BMP2 (Santa Cruz Biotechnology), VEGF (Santa Cruz Biotechnology), major histocompatibility complex I (MHC class I) (Santa Cruz Biotechnology), and human proliferating cell nuclear antigen (PCNA) (Dako, Glostrup, Denmark, http://www.dako.com) using the ABC (Vector Laboratories, Burlingame, CA, http://www.vectorlabs.com) method. All quantitative and structural morphometric data use nomenclature described by the American Society for Bone and Mineral Research Nomenclature Committee [23].

Statistical Analysis

Statistical analysis was performed using an appropriate analysis of variance when more than two groups were compared, followed by a post hoc Tukey's test to compare between groups. p values are indicated in the figures and figure legends.

Results

Human Adipose Tissue Contains Two Distinct Perivascular Cell Populations

We previously described, purified, and characterized two perivascular sources of primary MSCs within human adipose tissue on the basis of the expression of CD34 and CD146. Pericytes, which are surrounding microvessels, are isolatable from multiple adult organs, including adipose tissue, as CD45−, CD146+, CD34− cells [11, 16]. More recently, we described a second and distinct perivascular MSC population, CD45−, CD146−, CD34+ adventitial cells [17]. Here, we first confirmed our previous results, showing that pericytes (CD146+, CD34−) and adventitial cells (CD146−, CD34+) are distinct populations isolatable from human lipoaspirate after exclusion of DAPI+ cells (dead cells) and CD45+ cells (hematopoietic cells) (supplemental online Fig. 1).

Next, mean cell yield, viability, and frequency were examined across all samples (Fig. 1). In our experience with 60 samples, we have observed a somewhat variable total cell yield, as expressed in total hSVF cells per 100 ml of tissue lipoaspirate. Most commonly, total SVF cell yield fell within a range between 10×10^6 and 70×10^6 cells (mean, 39.4×10^6; median, 34.3×10^6) (Fig. 1A). Cell viability among SVF, as determined by DAPI− cells by flow cytometry, was above 70% in nearly all cases (mean, 81.2%; median, 89.8%) (Fig. 1B). Next, the prevalence of CD45+ cells was analyzed; the analysis was performed so as to exclude hematopoietic cells for hPSC isolation. CD45+ hematopoietic cells most commonly represented less than 40% of hSVF in nearly all cases (mean, 24.4%; median, 24.5%) (Fig. 1C). The two known perivascular stem cell populations were next analyzed: pericytes and adventitial cells. Pericytes most frequently represented 30% or less of total hSVF (mean, 19.5%; median, 16.7%) (Fig. 1D). Adventitial cells represented 40% or less of total hSVF (mean, 23.8%; median, 22.6%) (Fig. 1E). When added in combination, the total hPSC content most commonly fell between 30% and 60% of total viable hSVF (mean, 43.2%; median, 41.7%) (Fig. 1F). Conversely, non-hPSC CD45− cells represented a mean of 32.3% of total SVF.

Variation in Perivascular Stem Cell Yield by Cold-Storage Time

In a clinical setting, it may be very difficult to coordinate the harvest of liposuction with its immediate processing for cell isolation. In fact, in our research experience we found this to be the case, with samples being processed even more than 72 hours after liposuction. In such circumstances, refrigerated storage of lipoaspirate would be necessary. To determine the effects of cold storage, we stratified the data of cell yield, viability, and identity by hours of storage at 4°C (grouped per 24-hour period; Fig. 2). Total SVF cell yield showed a nonsignificant reduction after 72 hours (Fig. 2A). Remarkably, cell viability showed no difference even at 72+ hours, as determined by DAPI staining (Fig. 2B). Next, the prevalence of CD45+ hematopoietic cells was analyzed. A nonsignificant reduction in percentage of CD45+ cells

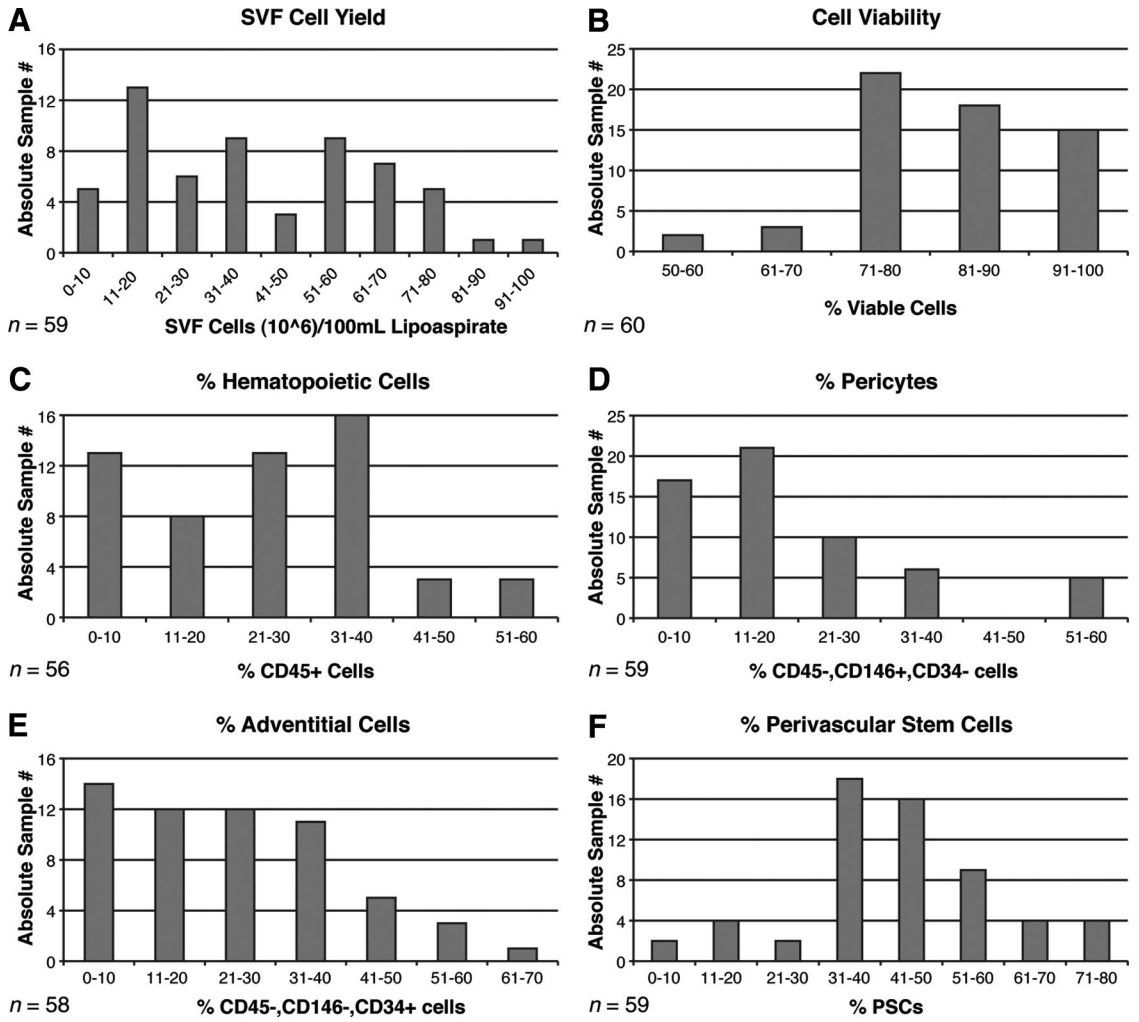

Figure 1. Yield, viability, and frequency of human PSCs in human white adipose tissue. **(A):** Total SVF cell yield, as represented by total SVF cells (10^6) per 100 ml of tissue lipoaspirate. Blood and saline of lipoaspirate fluid are not included in these calculations. Each bar indicates the number of lipoaspirate samples falling within the stated range of values. **(B):** Percentage of cell viability, as determined by percentage of DAPI− cells by flow cytometry. **(C):** Percentage of hematopoietic cells, as determined by percentage of CD45+ cells among viable (DAPI−) cells by flow cytometry. **(D):** Percentage of pericytes, as determined by percentage of CD146+, CD34− cells among viable (DAPI−) cells. **(E):** Percentage of adventitial cells, as determined by percentage of CD146−, CD34+ cells among viable (DAPI−) cells. **(F):** Percentage of human PSCs, as determined by percentage of pericytes + percentage of adventitial cells. Abbreviations: PSC, perivascular stem cell; SVF, stromal vascular fraction.

was observed across all time points greater than 24 hours of cold storage (Fig. 2C). The two known PSC populations, pericytes and adventitial cells, were then analyzed (Fig. 2D, 2E). Interestingly, pericytes showed a gradual increase in percentage prevalence with increasing time cold storage, ranging from 14.2% for those samples processed immediately to 28.3% for those processed more than 72 hours post-harvest (Fig. 2D). Conversely, adventitial cells showed a nonsignificant reduction in percentage prevalence with increasing time (Fig. 2E). Finally, the percentage prevalence of hPSCs was unchanged by hours of cold storage (Fig. 2F).

Variation in Perivascular Stem Cell Yield by Patient Demographics

Next, variation in cell yield, viability, and identity was analyzed by patient age, stratified by decade of life (Fig. 3). A nonsignificant reduction in cell viability was observed with patient age ≥51 (Fig. 3B). Percentage prevalence of pericytes showed a nonsignificant reduction with patient age >31 (Fig. 3D). In all respects, however, no significant change in yield, viability, or identity was observed with patient age.

Next, cell parameters of yield, viability, and identity were stratified by patient gender (Fig. 4A–4F). Mean SVF cell yield was significantly reduced in male patients as compared with female patients (Fig. 4A). No significant difference across genders was observed with cell viability, percentage of CD45+ cells, or percentage of pericytes (Fig. 4B–4D). Conversely, the percentage prevalence of adventitial cells and hPSCs was significantly increased among male patients (Fig. 4E, 4F).

Next, the effects of menopause were assessed on cell parameters of yield, viability, and identity (Fig. 4G–4L). For the purposes of this stratification, a mean age of menopause (51 years) was used as the partition to identify presumed menopausal status. Cell viability and percentage prevalence of adventitial cells were both nonsignificantly reduced among postmenopausal women (Fig. 4H, 4K), whereas the percentage prevalence of pericytes was nonsignificantly increased after menopause (Fig. 4J). Thus, menopausal status had no

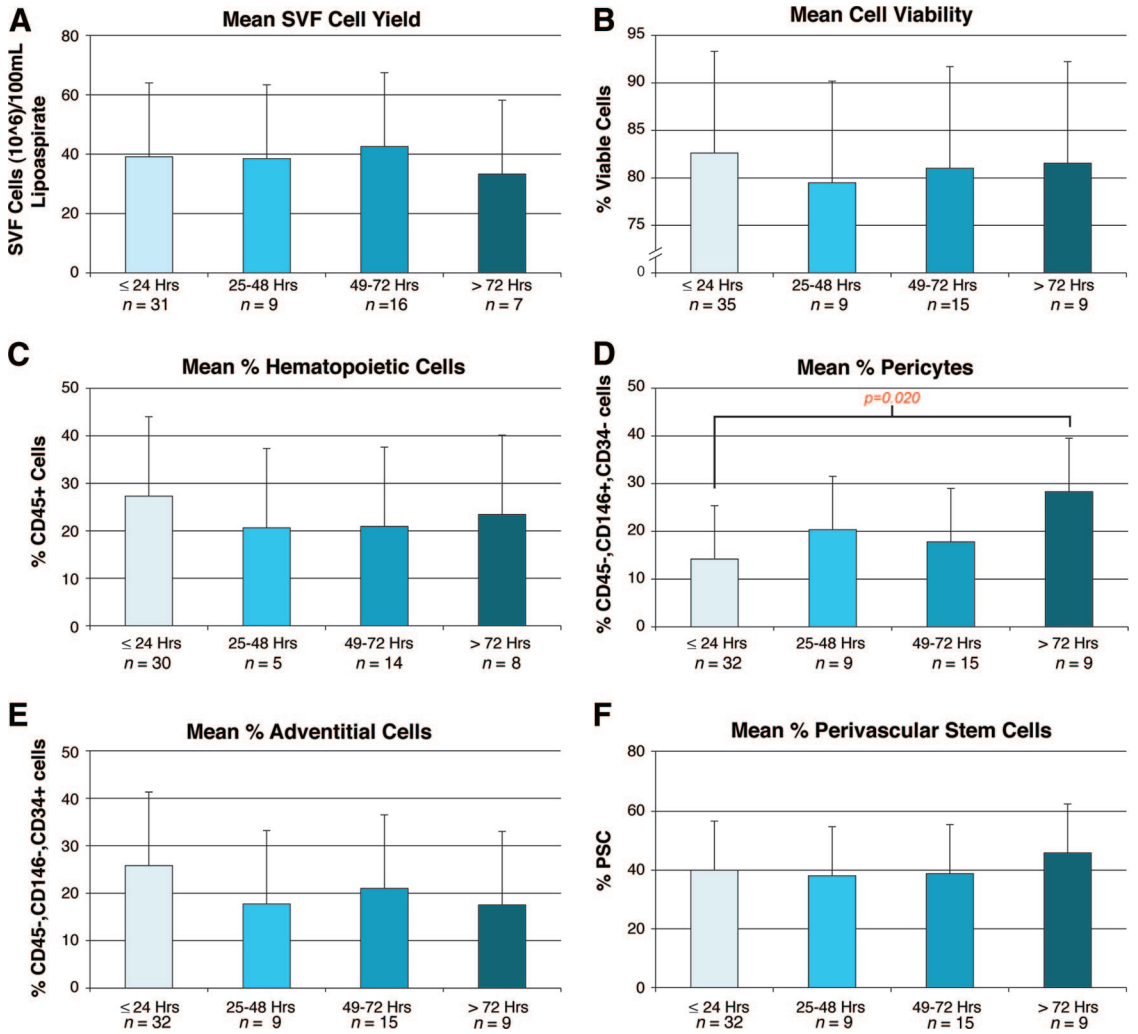

Figure 2. Effects of storage on human PSC yield, viability, and frequency. Samples were shipped and stored as unprocessed lipoaspirate at 4°C prior to digestion, staining, and fluorescence-activated cell sorting isolation. Characteristics of cell yield, viability, and frequency were assessed, stratified by hours of storage. Ranges of hours of storage were 0–24, 25–48, 49–72, and >72 hours, calculated from shipment to processing. Maximum storage time was 168 hours. **(A):** Total SVF cell yield, as represented by total SVF cells (10^6) per 100 ml of tissue lipoaspirate. **(B):** Percentage of cell viability, as determined by percentage of DAPI− cells. **(C):** Percentage of hematopoietic cells, as determined by percentage of CD45+ cells among DAPI− cells. **(D):** Percentage of pericytes, as determined by percentage of CD146+, CD34− cells among DAPI− cells. **(E):** Percentage of adventitial cells, as determined by percentage of CD146−, CD34+ cells among DAPI− cells. **(F):** Percentage of human PSCs, as determined by percentage of pericytes + percentage of adventitial cells. Abbreviations: PSC, perivascular stem cell; SVF, stromal vascular fraction.

statistically significant effects on any cell parameters of yield, viability, or identity.

Finally, patient samples were analyzed by BMI (Fig. 5). Patients were stratified by nonoverweight (BMI <25 kg/m^2), overweight (BMI 25–30 kg/m^2), and obese (BMI >30 kg/m^2). With increasing BMI, a nonsignificant trend was observed toward reduced SVF cell yield (Fig. 5A). The percentage prevalence of cells within SVF was observed to vary by BMI (Fig. 5C–5F). With increasing BMI, a trend toward increased frequency of hematopoietic cells and reduced frequency of pericytes and hPSCs was observed. Thus, BMI had clear (although not statistically significant) effects on cell yield and identity.

Collectively, changes in patient age, gender, and BMI led to infrequent and small changes in cell parameters of hPSC isolation. These data collected from $n = 60$ patients show evidence of reproducibility of hPSC isolation.

Human Perivascular Stem Cells Heal Critical-Sized Calvarial Defects

Having demonstrated the reproducibility of hPSC isolation, we next sought to define hPSC efficacy in bone healing. A critical-sized calvarial defect model was used (3-mm parietal bone, full-thickness defect). Importantly, a critical-sized bone defect represents one of the most challenging clinical scenarios for bone repair. For these experiments, scaffold seeded with either hPSCs or unsorted hSVF, from the same patient and at identical cell numbers, were implanted into defects ($n = 4$ separate patient samples used). A scaffold without cells served as a control. Osteoinductive scaffolds were composed of hydroxyapatite-coated PLGA as previously described [1, 2]. Details of scaffold composition and cell application can be found in supplemental online Table 2.

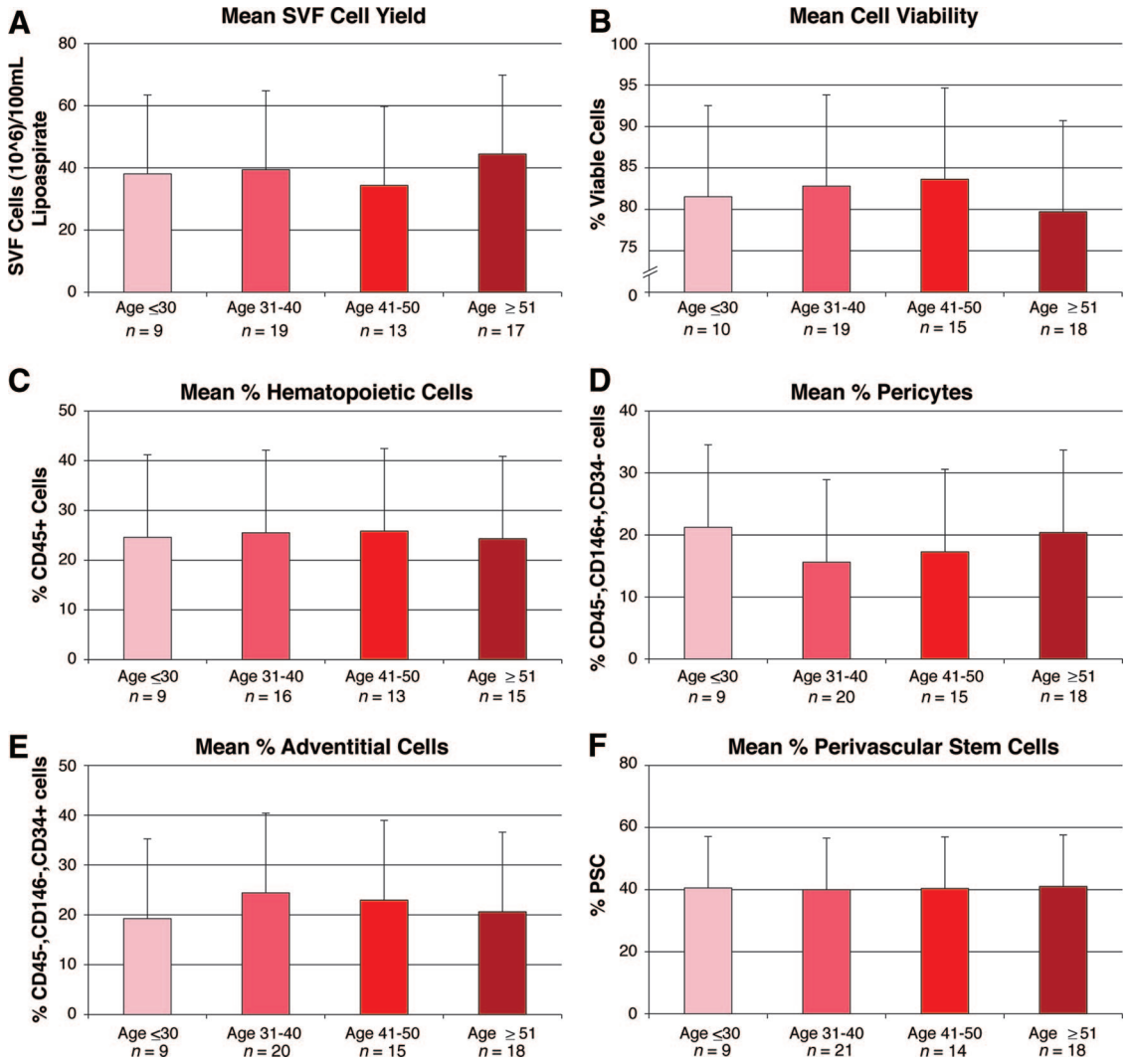

Figure 3. Effects of age on human PSC yield, viability, and frequency. Samples were derived from both genders and a wide range of ages (24–69 years). Characteristics of cell yield, viability, and frequency were assessed, stratified by age. Parameters of yield, viability, and frequency were as follows. **(A):** Total SVF cell yield, as represented by total SVF cells (10^6) per 100 ml of tissue lipoaspirate. **(B):** Percentage of cell viability, as determined by percentage of DAPI− cells. **(C):** Percentage of hematopoietic cells, as determined by percentage of CD45+ cells among DAPI− cells. **(D):** Percentage of pericytes, as determined by percentage of CD146+, CD34− cells among DAPI− cells. **(E):** Percentage of adventitial cells, as determined by percentage of CD146−, CD34+ cells among DAPI− cells. **(F):** Percentage of human PSCs, as determined by percentage of pericytes + percentage of adventitial cells. Abbreviations: PSC, perivascular stem cell; SVF, stromal vascular fraction.

hPSC-laden scaffolds led to significant defect reossification, whereas hSVF-laden scaffolds did not. This was observed by high-resolution microCT scanning and 3D reconstructions (Fig. 6A). Very little ossification was observed among scaffolds without cells (Fig. 6A, left). hSVF-seeded scaffolds led to scattered ossification (Fig. 6A, middle), whereas hPSC-treated scaffolds showed much more robust ossification by 8 weeks postoperative (Fig. 6A, right). Serial live microCT scans were performed every 2 weeks postoperative and were next quantified as percentage of healing of the original defect, using Photoshop (Adobe Systems Inc., San Jose, CA, http://www.adobe.com) (Fig. 6B). hSVF-seeded scaffolds led to minimal healing with no significant difference to scaffolds without cells. In contrast, hPSC-seeded scaffolds led to progressive reossification of the defect site (up to 61.5% and 69% healing at 4 and 6 weeks, respectively), significantly higher than either hSVF-seeded scaffolds or scaffolds without cells. Notably, defects without any treatment (without a scaffold) showed no defect reossification ($n = 3$ animals; data not shown).

Next, histologic examination of the calvarial defect site was performed after H&E and Masson's trichrome staining (Fig. 6C). Photographs were taken at the lateral defect edge. Upon treatment of either control scaffolds or SVF-seeded scaffolds, an abrupt cutoff was clear where the surgically created defect was performed (Fig. 6C, left and middle sections). In these samples, minimal scattered new osteoid formation was observed in serial sections (data not shown). In stark contrast, defects treated with hPSC-seeded scaffolds showed considerable new-formed bone (Fig. 6C, right section). In summary, hPSCs led to significant calvarial ossification, whereas patient-matched hSVF cells did not.

Finally, we next examined protein expression of various key osteogenic genes by immunohistochemistry. First, bone matrix

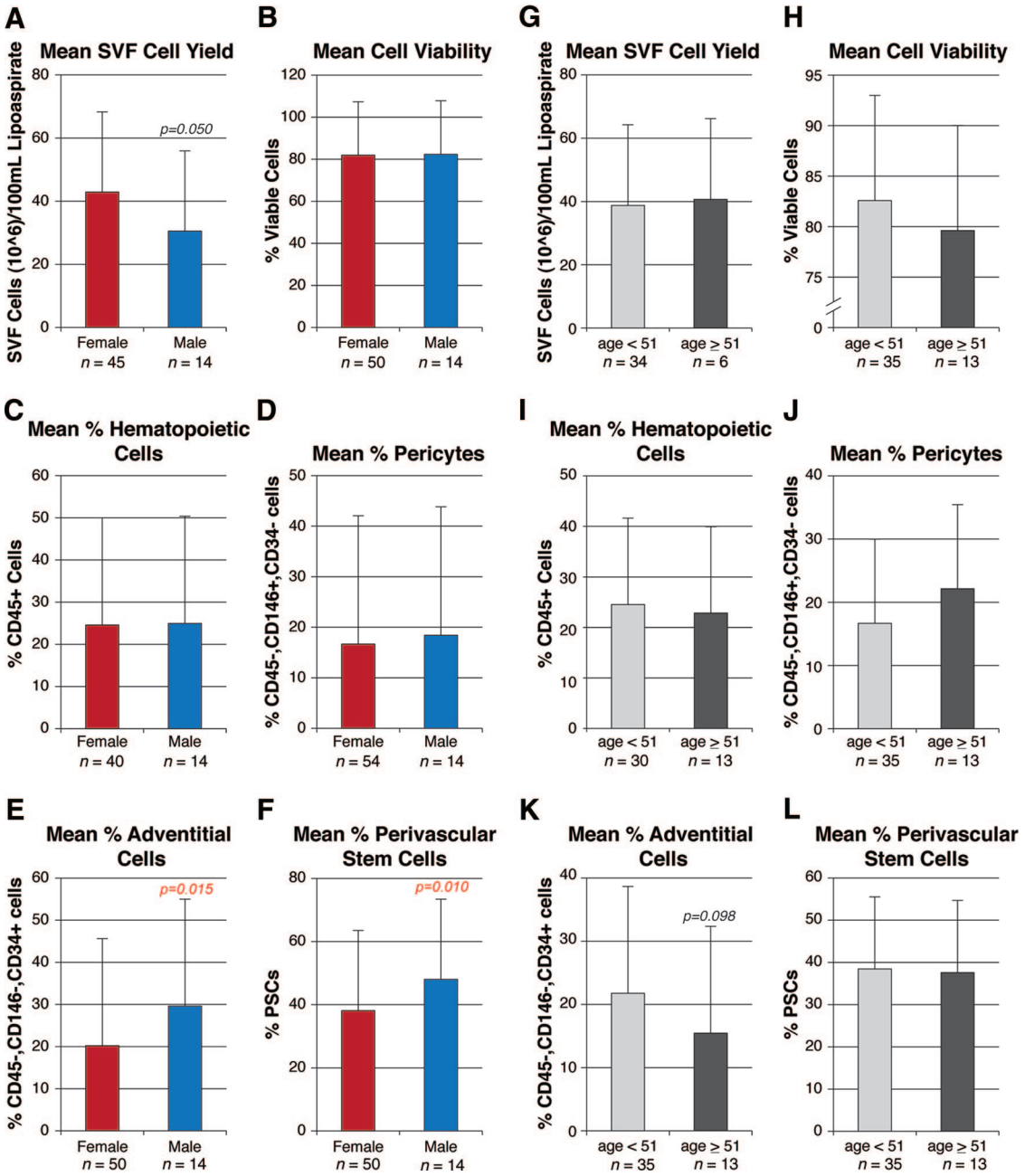

Figure 4. Effects of gender on human perivascular stem cell (hPSC) yield, viability, and frequency. Samples were derived from both genders and a wide range of ages (24–69 years). Characteristics of cell yield, viability, and frequency were assessed, stratified by either gender **(A–F)** or menopausal status **(G–L)**. Menopausal status was estimated on the basis of female age less than or greater than 51. Parameters of yield, viability, and frequency were as follows. **(A, G):** Total SVF cell yield, as represented by total SVF cells (10^6) per 100 ml of tissue lipoaspirate. **(B, H):** Percentage of cell viability, as determined by percentage of DAPI− cells. **(C, I):** Percentage of hematopoietic cells, as determined by percentage of CD45+ cells among DAPI− cells. **(D, J):** Percentage of pericytes, as determined by percentage of CD146+, CD34− cells among DAPI− cells. **(E, K):** Percentage of adventitial cells, as determined by percentage of CD146−, CD34+ cells among DAPI− cells. **(F, L):** Percentage of hPSCs, as determined by percentage of pericytes + percentage of adventitial cells. Abbreviations: PSC, perivascular stem cell; SVF, stromal vascular fraction.

protein expression, including OPN and OCN, was examined (Fig. 7A, 7B). Consistent with its role as an intermediate marker of osteogenesis [24], all three treatment groups showed numerous OPN+ cells. hPSC-treated scaffolds were the only treatment group, however, to show OPN+ bone-lining osteoblasts and OPN+ osteocytes within the defect site (Fig. 7A, far right). For OCN, consistent with its known role as a late marker of osteogenesis [25], a more scattered distribution of positive staining was observed. This was most predominant within osteoid present in hPSC-seeded scaffolds (Fig. 7B, right panels) and less frequent among scaffold and hSVF-seeded scaffold groups (Fig. 7B, left and middle panels). Next, two growth factors were examined: BMP2 and VEGF (Fig. 7C, 7D). Within scaffold only and hSVF-seeded scaffold groups, the cellular elements within the defect site were predominantly BMP2-negative, with only sporadic staining for VEGF (Fig. 7C, 7D, left and middle panels). In

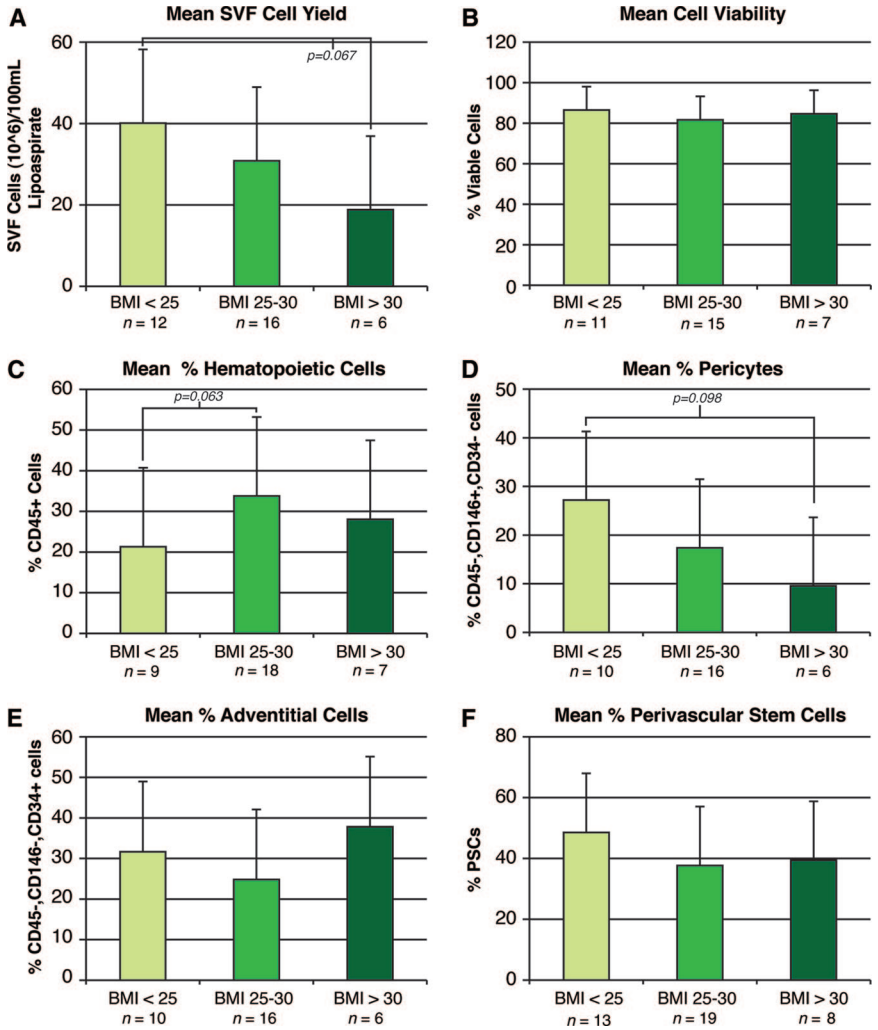

Figure 5. Effects of BMI on human perivascular stem cell (hPSC) yield, viability, and frequency. Samples were derived from nonoverweight (BMI <25 kg/m^2), overweight (BMI 25–30 kg/m^2), and obese (BMI >30 kg/m^2) patients. Characteristics of cell yield, viability, and frequency were stratified by patient BMI. **(A):** Total SVF cell yield. **(B):** Percentage of DAPI− cells. **(C):** Percentage of CD45+ hematopoietic cells. **(D):** Percentage of pericytes (CD146+, CD34− cells). **(E):** Percentage of adventitial cells (CD146−, CD34+ cells). **(F):** Percentage of hPSCs (pericytes + adventitial cells). Abbreviations: BMI, body mass index; PSC, perivascular stem cell; SVF, stromal vascular fraction.

stark contrast, cellular areas within the hPSC-treated scaffold group were intensely BMP2+, VEGF+ (Fig. 7C, 7D, right panels). Finally, we sought to confirm the persistence of human cells within the defect site, either by human MHC class I or anti-human PCNA immunohistochemistry (Fig. 7E, 7F). Indeed, we found persistence of human SVF or PSCs at 8 weeks postoperative (Fig. 7E, 7F). Interestingly, we observed greater staining for human markers in hPSC-seeded specimens, indicating improved proliferation and/or survival of hPSCs within the calvarial defect site.

Thus and in summary, despite the persistence of engrafted cells, hSVF was observed to be ineffective in inducing calvarial defect ossification, with minimal evidence of radiographic or histologic differences in comparison with scaffold without cells. In stark contrast, hPSCs induced significant increases in osteogenic growth factor elaboration (BMP2, VEGF); significant evidence of OPN+, OCN+ osteoblastogenesis; and ultimately significant calvarial defect reossification.

Discussion

Perivascular Cells as a Purified Stem Cell Source

For the first time, we have shown that a purified population of adipose-derived stem cells (hPSCs) is superior to unseparated hSVF for skeletal defect healing. hPSCs are an attractive cell source as they are plentiful within adipose tissue (constituting, on average, 43.2% of total viable hSVF). Given this prevalence of hPSCs, we would estimate that less than 200 ml of lipoaspirate would be sufficient starting material for the clinical application of hPSCs in localized bone repair. For example, 200 ml of lipoaspirate would theoretically yield 31 million cells, which by our estimates would be sufficient for healing of a 2-cm mid-diaphyseal femoral defect (cell seeding density of 1 million per 0.4 ml). With the increasing incidence of obesity in the U.S. and worldwide [26], the isolation of 200 ml of adipose tissue should be easily performed from all but the thinnest of patients. The yield and prevalence of hPSCs were minimally affected by all demographic

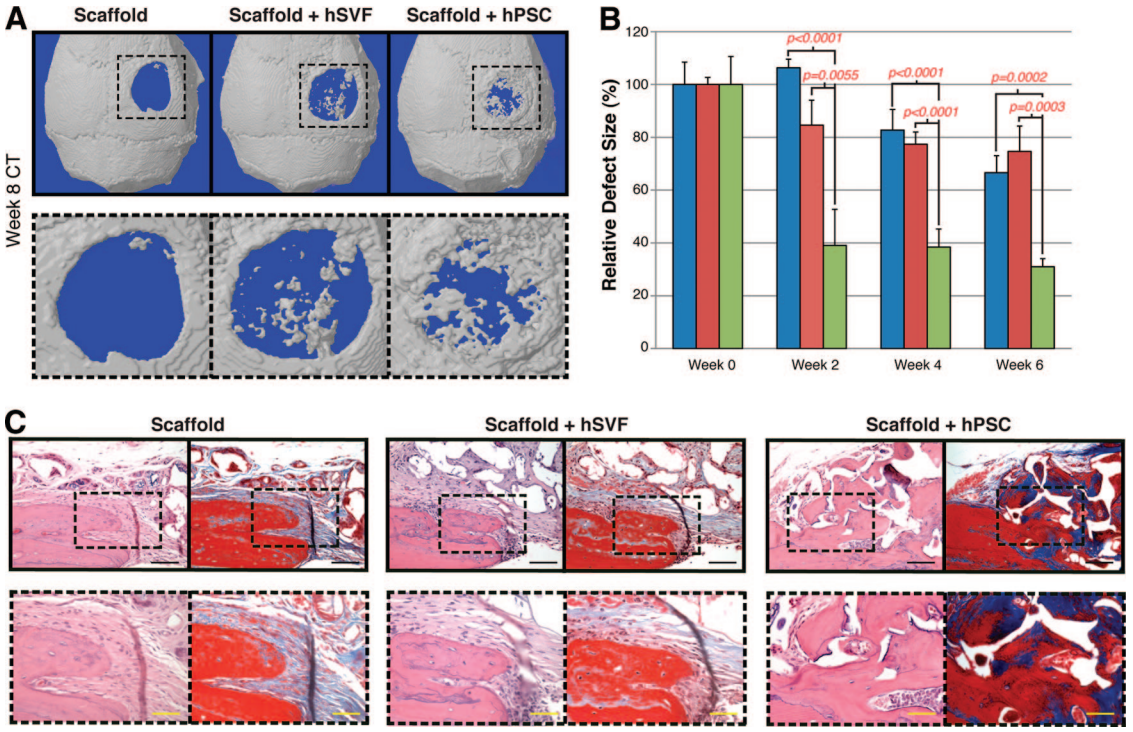

Figure 6. Calvarial healing by microCT and histology. hSVF or hPSCs were used to treat a 3-mm-diameter parietal bone defect in a SCID mouse. A custom-made hydroxyapatite-coated poly(lactic-coglycolic acid) scaffold was used as a carrier. Defects were treated with either an empty scaffold or a scaffold seeded with cells (scaffold + hSVF or scaffold + hPSC). Details of treatment groups are given in supplemental online Table 2. **(A):** Three-dimensional reconstructions of control, hSVF-treated, or hPSC-treated calvarial defects shown at 8 weeks postoperative. A CT threshold of 40 was used. **(B):** Relative defect healing as assessed by 0, 2, 4, and 6 weeks postoperative by serial live microCT scans. Relative defect area was calculated using a top-down view of the calvaria using AMIDE software images, followed by Adobe Photoshop quantification of relative defect size. **(C):** Representative hematoxylin/eosin and Masson's trichrome images for the defect site. Images are taken from the lateral defect edge to delineate old from new bone. $n = 16–18$ mice per treatment group split equally among $n = 4$ separate patient samples. Patient demographics are given in supplemental online Table 1. Black scale bars = 50 μm. Yellow scale bars = 25 μm. Abbreviations: CT, computed tomography; hPSC, human perivascular stem cell; hSVF, human stromal vascular fraction.

parameters examined, including patient age, gender, and body mass index. These observations, made from 60 distinct patient samples, suggest the high reproducibility of hPSC isolation for future clinical application.

Variations in Perivascular Stem Cell Yield

We analyzed the variation in PSC yield with differences in age, gender, and BMI. Remarkably, large variations were not observed with any of these demographics, suggesting that hPSCs could be isolated with success from virtually any patient. First, no statistically significant differences were observed with age. This was somewhat unexpected, as the vascularity of adipose and other tissue is reduced with patient age [27, 28]. However, those undergoing liposuction were only 24–69 years of age, and so with further extremes of patient age a significant impact in cell characterization may be appreciated. Second, stratification by gender was most remarkable for increased prevalence of adventitial cells and hPSCs among male liposuction specimens. Other research groups have found increased osteogenic differentiation among male ASCs [29, 30], and it is most likely that this in fact represents an increased prevalence of hPSCs. Third, some investigators have noted a reduction in stem cell numbers with the onset of menopause [31]; however, our analysis of pre- and postmenopausal liposuction samples did not find any significant association. However, our calculations were based on a mean age of menopause (age 51) rather than a clinical history. Thus, future studies should obtain individual menopausal status of the patient to confirm our findings. Finally, we observed that increasing BMI was associated with reduced cell yield, reduced prevalence of pericytes, and increased prevalence of hematopoietic cells, although all results failed to achieve statistical significance. The trend toward increased prevalence of CD45+ hematopoietic cells is consistent with other reports linking high BMI with inflammation [32–34]. In addition, a trend toward a reduction in pericyte numbers was observed. This is also in agreement with previous reports showing reduced capillary numbers in adipose tissue of obese patients [35]. In summary, although the cell parameters showed small changes with patient demographics, these changes are not without some substantiation in the literature.

Resilience of Pericytes in Cold Storage

Samples were stratified by the hours of refrigerated storage between initial surgical isolation and subsequent laboratory-based processing. Taking into account all samples processed, the mean cold-storage delay from isolation to processing was 49 ± 35.7 hours (mean ± SD; median, 48 hours). Surprisingly, the major finding with stratification of hours in cold storage was an association between increasing cold-storage time and an increasing prevalence of pericytes. If this association is indeed causal, two possible theories would explain this phenomenon. First, the effects of hypoxia on perivascular stem cells have been previously

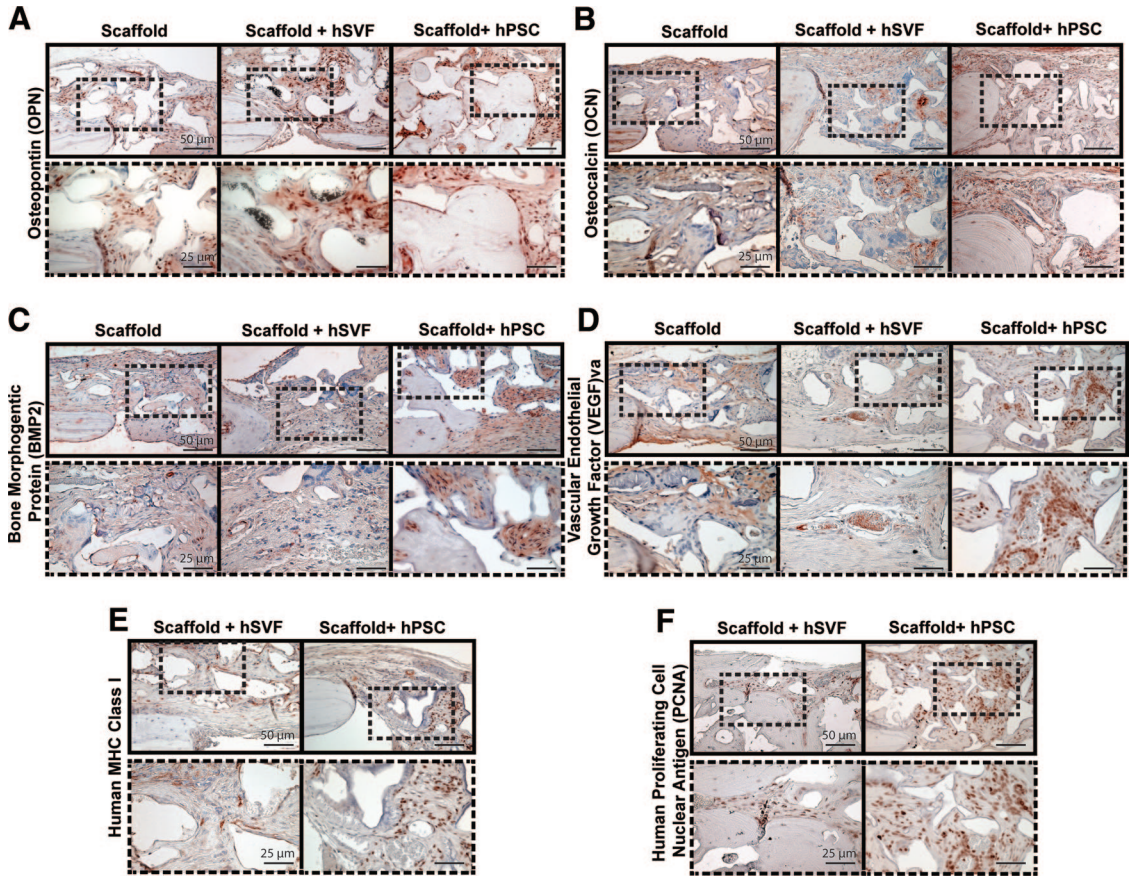

Figure 7. Calvarial healing by immunohistochemistry. hSVF or hPSCs were used to treat a 3-mm-diameter parietal bone defect in a SCID mouse. A custom-made hydroxyapatite-coated poly(lactic-coglycolic acid) scaffold was used as a carrier. Defects were treated either with an empty scaffold or with a scaffold seeded with hSVF or hPSCs. Treatment groups are given in supplemental online Table 2. Immunostaining was performed for OPN **(A)**, OCN **(B)**, BMP2 **(C)**, VEGF **(D)**, MHC class I **(E)**, and PCNA **(F)**. $n = 16–18$ mice per treatment group split equally among $n = 4$ separate patient samples. Scale bars = 50 μm (top rows), 25 μm (bottom rows). Abbreviations: BMP2, bone morphogenetic protein 2; hPSC, human perivascular stem cell; hSVF, human stromal vascular fraction; MHC, major histocompatibility complex; OCN, osteocalcin; OPN, osteopontin; PCNA, proliferating cell nuclear antigen; VEGF, vascular endothelial growth factor.

examined in detail [36]. Remarkably, human pericytes exposed to hypoxia showed increased DNA synthesis, proliferation, and migration (6% vs. 21% O_2). Thus, the increasing prevalence of pericytes with time in storage may reflect a relative hardiness to hypoxic conditions. Alternatively, pericytes are intimately associated with endothelial cells, whereas adventitial cells are more loosely connected. Prolonged hypoxic cold storage may allow for more ready dissociation of pericytes from the vasculature, so that by cell sorting, a higher prevalence of dissociated PSCs is obtained. In either event, prolonged hours of cold storage may not be detrimental for future tissue engineering applications using adipose-derived hPSCs.

Mechanisms of hPSC-Mediated Calvarial Defect Reossification

In coordination with our analysis of lipoaspirates to determine cell yield, viability, and identity, we also used a calvarial defect model to evaluate hPSC efficacy for skeletal defect reossification. In a previous publication, we had definitively observed that hPSCs had increased in vivo bone formation potential in comparison with patient-matched hSVF [20]. This comparison was performed in an intramuscular (ectopic) bone model, which is very different from a bone defect model. Here, we extended these findings to a nonhealing calvarial bone defect, finding increased reossification following hPSC treatment. Ossification occurred principally through intramembranous ossification, as no cartilage was observed within defect sites. However, previous studies have observed PSCs to participate in cartilage differentiation [11, 17], and endochondral ossification as well [37]. The mechanisms of improved hPSC osteogenesis are only partially elucidated. These include three interrelated hypotheses: (a) the relative purity of MSCs within the hPSC population, (b) the elimination of non-MSC cell types, and (c) improved trophic effects from hPSCs. First, as mentioned, both subpopulations of hPSCs have been shown by clonal analysis to be purified ancestors of MSCs. Thus, sorting for hPSC markers ensures a highly purified MSC population for implantation, whereas non-hPSCs (either CD45−, CD34−, CD146− or CD45−, CD34+, CD146+) do not have MSC-like characteristics [17]. Next, there exists precedent to suggest that endothelial cells may actually inhibit MSC osteogenesis. For example, endothelial cells have been described to negatively regulate the differentiation of MSCs, such as ASCs or bone marrow mesenchymal stem cells (BMSCs) [38, 39]. For instance, human endothelial cells inhibit BMSC differentiation into mature osteoblasts by interfering with Osterix expression [39]. With this evidence in mind, hPSCs (which are CD31−) may show enhanced bone formation in part by elimination of the endothelial cell component. Finally, hPSCs may show such robust bone induction

through a trophic effect on endogenous cell types. For example, previous studies have also shown that hPSCs secrete more osteogenic and vasculogenic growth factors, such as VEGF, platelet-derived growth factor, and fibroblast growth factor-2, than do ASCs [15, 37]. Here, we confirmed that hPSC-treated calvarial defects show increased expression of VEGF and BMP2 compared with corresponding hSVF-treated defects. hPSC elaboration of VEGF also brings to the fore the point that hPSCs may also stimulate bone growth via positive effects on vasculogenesis. Indeed, hPSCs are known to maintain endothelial cell function [40, 41], and the provasculogenic effects of hPSCs in the context of bone formation are the subject of ongoing studies.

Conclusion

These data show that hPSCs are readily obtainable from human lipoaspirate in sufficient quantities for future clinical efforts in skeletal tissue regeneration. PSCs show high reproducibility of isolation from adipose tissue, as cell yield, viability, and frequency are minimally affected by patient age, gender, or BMI. Uncultured hPSCs show superiority to patient-matched, unpurified hSVF with respect to the quantity and quality of bone regeneration. From the perspective of regulatory approval by the U.S. Food and Drug Administration (FDA), hPSCs are a potentially readily approvable stem cell technology. Variability in cell composition presents disadvantages for FDA approval of a future stem cell-based therapeutic, potentially including reduced safety, purity, identity, potency, and efficacy. Notably, these are the criteria upon which the Center for Biologics Evaluation and Research evaluates stem cell-based product applications [42]. For example, given the heterogeneity of SVF, precise product characterization is not feasible, leading to lack of hSVF product identity. Batch-to-batch variability and nonuniformity in effect (again attributable to variable stem cell content) reduce the efficacy and potency of hSVF compounds and potentially reduce product safety. Thus, the regulatory hurdles for hPSC approval may likely be lower than for other traditional cell types.

In fact, bone tissue is not the area of hPSC-mediated tissue regeneration to show promise. Excitingly, recent studies have already demonstrated the utility of hPSCs for regeneration of disparate tissue types, including skeletal muscle [43], lung [44], and even myocardium [16]. Thus, from both efficacy and safety standpoints, hPSCs may represent a new and attractive MSC progenitor cell source for tissue regeneration.

Acknowledgments

We thank Jessica Scholes and Felica Codrea in the Broad Stem Cell Research Center FACS core, the Crump Institute for Molecular Imaging, the Translational Pathology Core Laboratory and Surgical Pathology divisions of the Department of Pathology and Laboratory Medicine (University of California, Los Angeles), and the following individuals for the excellent technical assistance: Raghav Goyal, Angel Pan, Leslie Chang, Todd Rackohn, Donnalisa Soofer, Virginia Nguyen, and Dr. Sonja Lobo. This work was supported by California Institute for Regenerative Medicine (CIRM) Early Translational II Research Award TR2-01821, NIH/National Institute of Dental and Craniofacial Research Grant R21 DE0177711, T32 training fellowship 5T32DE007296-14 (to A.W.J.), and CIRM Training Grant Research Fellowship TG-01169 (to M.C. and J.N.Z.).

Author Contributions

A.W.J. and J.N.Z.: conception and design, collection and/or assembly of data, data analysis and interpretation, manuscript writing; M.C. and A.M.Z.: collection and/or assembly of data, data analysis and interpretation, manuscript writing; A.A., A.H., A.N., S.M., S.P., and X.Z.: collection and/or assembly of data, data analysis and interpretation; G.A.: collection of data, data analysis and interpretation; D.S.: provision of study material; B.W. and K.T.: financial support, administrative support, manuscript writing; B.P. and C.S.: conception and design, financial support, administrative support, manuscript writing, final approval of manuscript.

Disclosure of Potential Conflicts of Interest

K.T., B.P., and C.S. are inventors of perivascular stem cell-related patents filed from University of California, Los Angeles. K.T. and C.S. are founders of Scarless Laboratories Inc., which sublicenses perivascular stem cell-related patents from the University of California Regents, which also hold equity in the company. C.S. is also an officer of Scarless Laboratories, Inc., and a shareholder and consultant for Bone Biologics. X.Z. is a consultant with and holds intellectual property rights with Bone Biologics.

References

1 Levi B, James AW, Nelson ER et al. Human adipose derived stromal cells heal critical size mouse calvarial defects. PLoS One 2010;5:e11177.

2 Levi B, James AW, Nelson ER et al. Human adipose-derived stromal cells stimulate autogenous skeletal repair via paracrine hedgehog signaling with calvarial osteoblasts. Stem Cells Dev 2011;20:243–257.

3 Cui L, Liu B, Liu G et al. Repair of cranial bone defects with adipose derived stem cells and coral scaffold in a canine model. Biomaterials 2007;28:5477–5486.

4 Tapp H, Hanley EN, Jr., Patt JC et al. Adipose-derived stem cells: Characterization and current application in orthopaedic tissue repair. Exp Biol Med (Maywood) 2009;234:1–9.

5 Safwani WK, Makpol S, Sathapan S et al. The impact of long-term in vitro expansion on the senescence-associated markers of human adipose-derived stem cells. Appl Biochem Biotechnol 2012;166:2101–2113.

6 Gad SC. Pharmaceutical Manufacturing Handbook: Regulations and Quality. Hoboken, NJ: John Wiley & Sons, 2008.

7 Dahl JA, Duggal S, Coulston N et al. Genetic and epigenetic instability of human bone marrow mesenchymal stem cells expanded in autologous serum or fetal bovine serum. Int J Dev Biol 2008;52:1033–1042.

8 Müller AM, Mehrkens A, Schafer DJ et al. Towards an intraoperative engineering of osteogenic and vasculogenic grafts from the stromal vascular fraction of human adipose tissue. Eur Cell Mater 2010;19:127–135.

9 Cheung WK, Working DM, Galuppo LD et al. Osteogenic comparison of expanded and uncultured adipose stromal cells. Cytotherapy 2010;12:554–562.

10 Paredes B, Santana A, Arribas MI et al. Phenotypic differences during the osteogenic differentiation of single cell-derived clones isolated from human lipoaspirates. J Tissue Eng Regen Med 2011;5:589–599.

11 Crisan M, Yap S, Casteilla L et al. A perivascular origin for mesenchymal stem cells in multiple human organs. Cell Stem Cell 2008;3:301–313.

12 Crisan M, Huard J, Zheng B et al. Purification and culture of human blood vessel-associated progenitor cells. Curr Protoc Stem Cell Biol 2008;Chapter 2:Unit 2B.2.1–2B.2.13.

13 Crisan M, Deasy B, Gavina M et al. Purification and long-term culture of multipotent progenitor cells affiliated with the walls of human blood vessels: Myoendothelial cells and pericytes. Methods Cell Biol 2008;86:295–309.

14 Corselli M, Chen CW, Crisan M et al. Perivascular ancestors of adult multipotent stem cells. Arterioscler Thromb Vasc Biol 2010; 30:1104–1109.

15 Chen CW, Montelatici E, Crisan M et al. Perivascular multi-lineage progenitor cells in human organs: Regenerative units, cytokine sources or both? Cytokine Growth Factor Rev 2009;20:429–434.

16 Crisan M, Chen CW, Corselli M et al. Perivascular multipotent progenitor cells in human organs. Ann NY Acad Sci 2009;1176:118–123.

17 Corselli M, Chen CW, Sun B et al. The tunica adventitia of human arteries and veins as a source of mesenchymal stem cells. Stem Cells Dev 2012;21:1299–1308.

18 Levi B, Wan DC, Glotzbach JP et al. CD105 protein depletion enhances human adipose-derived stromal cell osteogenesis through reduction of transforming growth factor beta1 (TGF-beta1) signaling. J Biol Chem 2011;286: 39497–39509.

19 Jiang T, Liu W, Lv X et al. Potent in vitro chondrogenesis of CD105 enriched human adipose-derived stem cells. Biomaterials 2010; 31:3564–3571.

20 James AW, Zara J, Zhang X et al. Perivascular stem cells: A prospectively purified mesenchymal stem cell population for bone tissue engineering. Stem Cells Translational Medicine 2012;1:510–519.

21 Levi B, Nelson ER, Li S et al. Dura mater stimulates human adipose-derived stromal cells to undergo bone formation in mouse calvarial defects. Stem Cells 2011;29:1241–1255.

22 Hsu WK, Virk MS, Feeley BT et al. Characterization of osteolytic, osteoblastic, and mixed lesions in a prostate cancer mouse model using 18F-FDG and 18F-fluoride PET/CT. J Nucl Med 2008;49:414–421.

23 Parfitt AM, Drezner MK, Glorieux FH et al. Bone histomorphometry: Standardization of nomenclature, symbols, and units. Report of the ASBMR Histomorphometry Nomenclature committee. J Bone Miner Res 1987;2: 595–610.

24 Zohar R, Cheifetz S, McCulloch CA et al. Analysis of intracellular osteopontin as a marker of osteoblastic cell differentiation and mesenchymal cell migration. Eur J Oral Sci 1998;106(suppl 1):401–407.

25 Akahane M, Ueha T, Dohi Y et al. Secretory osteocalcin as a nondestructive osteogenic marker of tissue-engineered bone. J Orthop Sci 2011;16:622–628.

26 Mitchell NS, Catenacci VA, Wyatt HR et al. Obesity: Overview of an epidemic. Psychiatr Clin North Am 2011;34:717–732.

27 Herpin P, Lossec G, Schmidt I et al. Effect of age and cold exposure on morphofunctional characteristics of skeletal muscle in neonatal pigs. Pflugers Arch 2002;444:610–618.

28 Nnodim JO. Stereological assessment of age-related changes in lipid droplet surface area and vascular volume in rat interscapular brown adipose tissue. Anat Rec 1988;220:357–363.

29 Aksu AE, Rubin JP, Dudas JR et al. Role of gender and anatomical region on induction of osteogenic differentiation of human adipose-derived stem cells. Ann Plast Surg 2008;60: 306–322.

30 Yu G, Wu X, Dietrich MA et al. Yield and characterization of subcutaneous human adipose-derived stem cells by flow cytometric and adipogenic mRNA analyzes. Cytotherapy 2010; 12:538–546.

31 Narod SA. A model for breast cancer risk based on stem-cell theory. Curr Oncol 2012;19: 9–11.

32 Lessard A, Almeras N, Turcotte H et al. Adiposity and pulmonary function: Relationship with body fat distribution and systemic inflammation. Clin Invest Med 2011;34:E64–E70.

33 Honda H, Qureshi AR, Axelsson J et al. Obese sarcopenia in patients with end-stage renal disease is associated with inflammation and increased mortality. Am J Clin Nutr 2007; 86:633–638.

34 Beddhu S, Ramkumar N, Samore MH. The paradox of the "body mass index paradox" in dialysis patients: Associations of adiposity with inflammation. Am J Clin Nutr 2005;82: 909–910, author reply 910–911.

35 Spencer M, Unal R, Zhu B et al. Adipose tissue extracellular matrix and vascular abnormalities in obesity and insulin resistance. J Clin Endocrinol Metab 2011;96:E1990–E1998.

36 Tottey S, Corselli M, Jeffries EM et al. Extracellular matrix degradation products and low-oxygen conditions enhance the regenerative potential of perivascular stem cells. Tissue Eng Part A 2011;17:37–44.

37 Zhang X, Peault B, Chen W et al. The Nell-1 growth factor stimulates bone formation by purified human perivascular cells. Tissue Eng Part A 2011;17:2497–2509.

38 Rajashekhar G, Traktuev DO, Roell WC et al. IFATS collection: Adipose stromal cell differentiation is reduced by endothelial cell contact and paracrine communication: Role of canonical Wnt signaling. Stem Cells 2008;26:2674–2681.

39 Meury T, Verrier S, Alini M. Human endothelial cells inhibit BMSC differentiation into mature osteoblasts in vitro by interfering with osterix expression. J Cell Biochem 2006;98: 992–1006.

40 Schor AM, Allen TD, Canfield AE et al. Pericytes derived from the retinal microvasculature undergo calcification in vitro. J Cell Sci 1990;97:449–461.

41 Canfield AE, Doherty MJ, Wood AC et al. Role of pericytes in vascular calcification: A review. Z Kardiol 2000;89(suppl 2):20–27.

42 Lanza R, Gearhart J, Hogan B et al., eds. Essentials of Stem Cell Biology. Oxford, United Kingdom: Elsevier, 2009.

43 Park TS, Gavina M, Chen CW et al. Placental perivascular cells for human muscle regeneration. Stem Cells Dev 2011;20:451–463.

44 Montemurro T, Andriolo G, Montelatici E et al. Differentiation and migration properties of human foetal umbilical cord perivascular cells: Potential for lung repair. J Cell Mol Med 2011;15:796–808.

See www.StemCellsTM.com for supporting information available online.